Available online at www.sciencedirect.com
ScienceDirect
Nuclear Instruments and Methods in Physics Research A 582 (2007) 629–637
NUCLEAR INSTRUMENTS & METHODS IN PHYSICS RESEARCH Section A
www.elsevier.com/locate/nima

Monte Carlo and analytical models of neutron detection with organic scintillation detectors

Sara A. Pozzi[a], Marek Flaska[a,*], Andreas Enqvist[b], Imre Pázsit[b]

[a]*Oak Ridge National Laboratory, P.O. Box 2008, Oak Ridge, TN 37831-6010, USA*
[b]*Chalmers University of Technology, Chalmers, Sweden*

Received 2 July 2007; received in revised form 17 August 2007; accepted 29 August 2007
Available online 14 September 2007

Abstract

This paper presents a new technique for the analysis of neutron pulse height distributions generated in an organic scintillation detector. The methodology presented can be applied to techniques such as neutron spectrum unfolding, which have a variety of applications, including nuclear nonproliferation and homeland security. The technique is based on two independent approaches: (i) the use of the MCNP-PoliMi code to simulate neutron detection on an event-by-event basis with the Monte Carlo method and (ii) an analytical approach for neutron slowing down and detection processes. We show that the total neutron pulse height response measured by the organic scintillators is given by the sum of a large number of different neutron histories, each composed of a certain number of neutron scatterings on hydrogen and/or carbon. The relative contributions of each of these histories are described for a cylindrical liquid scintillator BC-501A. Simulations and measurements of neutron pulse height distributions are essential for neutron spectrum unfolding procedures.

PACS: 29.40Mc; 28.20Cz

Keywords: MCNP-PoliMi; Neutron detection; Organic scintillator; Pulse height distribution

1. Introduction

Organic scintillation detectors, in both liquid and plastic form, are widely used in detection systems for the identification and characterization of nuclear materials in applications such as nuclear nonproliferation, homeland security, and basic physics research. Studies describing the energy calibration of these types of detectors have been published in the literature since the 1960s. A good overview of both liquid and plastic scintillation counting can be found in Ref. [1]. Scintillation detectors are sensitive to both fast neutrons and gamma rays; pulse shape discrimination techniques can be applied to reject the gamma rays when neutron pulse analysis is required [2,3].

Neutron detection occurs by multiple scatterings on hydrogen (H) and/or carbon (C), the main constituents of the scintillator. At each interaction, the neutron deposits a portion of its initial energy until it escapes the detector or is captured. The former is more probable than the latter for neutrons in the million electron volts (MeV) range and detectors of up to several centimeters in size. The energy deposited by the neutron in the scattering collisions is then converted to scintillation light, which is collected by the photomultiplier tube and converted to a measured pulse. In general, the light produced is proportional to the amount of energy deposited by the neutron. However, because the conversion from energy to light is nonlinear and strongly dependent on the type of the secondary charged particle, the statistics of the individual neutron histories is important for understanding the mechanism of neutron

*Corresponding author. Tel.: +1 865 5745486.
E-mail addresses: pozzisa@ornl.gov (S.A. Pozzi), flaskam@ornl.gov, marek.flaska@yahoo.com (M. Flaska), andreas@nephy.chalmers.se (A. Enqvist), imre@nephy.chalmers.se (I. Pázsit).

0168-9002/$ - see front matter © 2007 Elsevier B.V. All rights reserved.
doi:10.1016/j.nima.2007.08.246

detection. This information is also important for performing unfolding procedures aimed at accurately determining the incident neutron spectrum.

Because neutron response functions vary with the composition and size of the scintillators, many papers can be found in the literature that describe specific calibration procedures performed for a given experimental setup. Past studies have reported neutron detection efficiency measurements for several detector types and incident neutron energies [3–9]. Other studies have compared experimental results with Monte Carlo predictions performed with modifications of the MCNP code [10,11].

One advantage of the proposed approach is that our code system allows the modeling of any material in any geometry, allowing the user to simulate the entire experimental system, including the source, fissile material, shielding, and detectors, without resorting to approximations or multistep calculations. This capability is a considerable improvement over previously-developed codes, such as SCINFUL [12], where (i) the simulation space is limited to the detector itself (with the detector being limited to cylindrical dimensions), (ii) the incident neutron spectrum is limited to monoenergetic or uniform and Maxwellian continuous spectra, and (iii) the individual neutron histories cannot be resolved. It should also be mentioned that the code system presented in this paper can calculate not only detector responses to incident neutrons, but also to gamma rays.

Whereas the detectors cannot resolve the individual neutron histories, Monte Carlo and analytical techniques can be used to split the total response into the individual contributions. A first attempt of this type of analysis was reported by Hermsdorf et al. [13]. The present paper extends that analysis and includes an analytical derivation of the light generated by the detector. Specifically, we present the results of such analysis for a few monoenergetic neutron sources and two continuous neutron sources (Cf-252 and Am-Be). To our knowledge, this type of detector analysis has not been reported in the past.

This paper is organized as follows: Section 2 gives the Monte Carlo methodology, Section 3 describes the simulation results, Section 4 presents the results from the analytical approach, and Section 5 gives conclusions.

2. Description of Monte Carlo simulations

Event-resolved predictions of the interactions of fast neutrons within the organic scintillator are performed using the code MCNP-PoliMi [14]. A specifically designed postprocessing code is used to determine the number of elastic collisions that the neutrons undergo with the H and C nuclei in the detector. The codes also allow us to calculate the amount of energy deposited in the detector in the single neutron interactions. Thus, the detector pulse height distributions can be calculated as a function of the n and m scatterings on H and C, respectively. It should be noted that these pulse height distributions depend not only on the n and m scatterings on H and C, but also on the order of these scatterings, as is shown in the following.

A cylindrical liquid scintillation detector with a height of 7.6 cm and diameter of 11.7 cm was used in the simulations. The H and C nuclei were the only nuclei modeled in the scintillation part of the detector, with a H:C ratio of 0.548:0.452. This composition corresponds to that of the liquid scintillator BC-501A manufactured by Saint-Gobain and is equivalent to the NE213 liquid scintillator. Separate simulations were performed for several monoenergetic neutron sources and for two continuous-energy neutron sources: Cf-252 and Am-Be.

The MCNP-PoliMi output files record every neutron interaction that occurs in the detector volume, including interaction type, energy deposited, and collision nucleus. The energy deposited is then converted into light output, taking into account the type of collision nucleus. In the case of scattering on H, the relationship between the energy deposited (T, in MeV) and the light output (L, in MeVee) is

$$L = aT^2 + bT \equiv L(T), \tag{1}$$

where $a = 0.035\,\mathrm{MeVee/MeV^2}$ and $b = 0.141\,\mathrm{MeVee/MeV}$ for liquid scintillators. This relation was acquired using experimental results [15].

In the case of scattering on C, the light output is very small. For this study the following relationship was used:

$$L(T) = cT, \tag{2}$$

where $c = 0.02\,\mathrm{MeVee/MeV}$ [11]. It is clear that the relations given by Eqs. (1) and (2) are simplified and empirical. In fact, the relations take into account in a crude manner many physical mechanisms such as the light spectrum emitted by the scintillator, the light emission and absorption by the scintillator and the scintillator's walls, the response of the photocathode, and the multiplication by the photomultiplier tube. Similar approximate treatments have been adopted in the past and have proven to be sufficient for most applications [3,13].

The amounts of light generated in single collisions on H and C were tallied separately, as well as the light outputs created in multiple collisions. For the particle histories consisting of multiple collisions, the order of the interactions was taken into account. Finally, the pulse height distributions for each of these possible histories were generated.

3. Monte Carlo results

Monoenergetic neutron sources were simulated with energies 1, 1.5, and 2 MeV. Fig. 1 shows the simulated pulse height distributions for 1 MeV incident neutrons. The possible neutron histories consisting of up to 3 collisions on H and C are shown in Table 1. It also shows the relative probabilities of these neutron histories for all 3 incident neutron energies. For example, it is implicitly shown in Table 1 that for all 3 incident neutron energies multiple

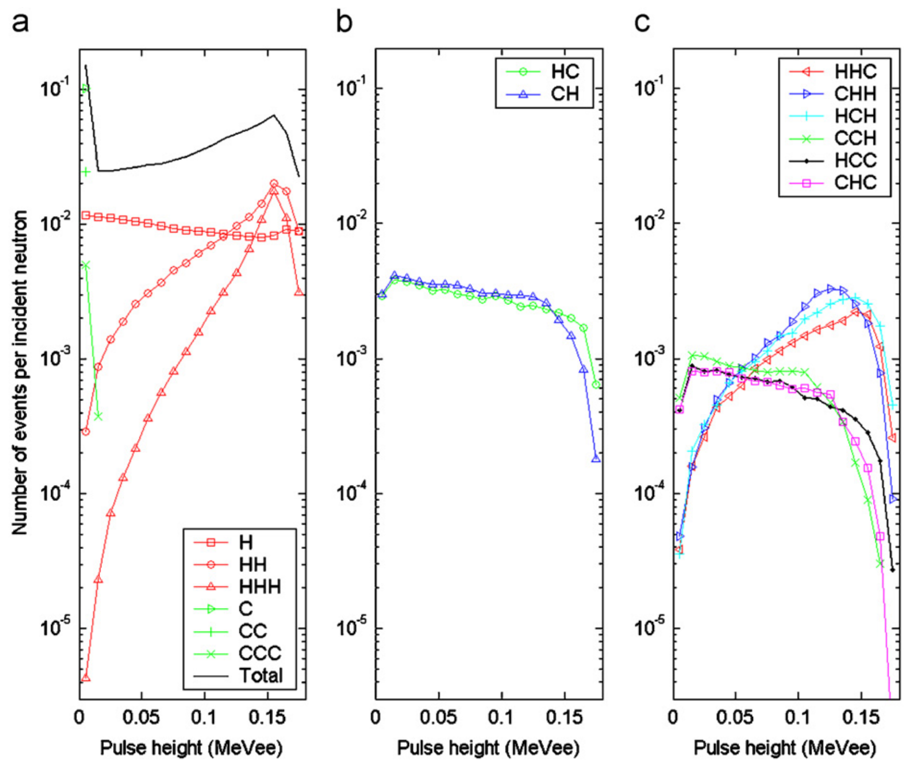

Fig. 1. Pulse height distributions from 1 MeV incident neutrons generated by neutron histories with (a) up to three scatterings on H or C only, (b) a single scattering on H and C, and (c) three scatterings on H and C.

Table 1
Collision history types and corresponding probabilities and relative errors

History type	Relative probability $E = 1$ MeV	Relative probability $E = 1.5$ MeV	Relative probability $E = 2$ MeV
No collision	1.9850E-01 ± 5.00E-04	2.5800E-01 ± 6.00E-04	3.0790E-01 ± 7.00E-04
H	1.7050E-01 ± 5.00E-04	1.7240E-01 ± 5.00E-04	1.7500E-01 ± 5.00E-04
HH	1.2650E-01 ± 4.00E-04	1.0930E-01 ± 4.00E-04	9.7447E-02 ± 4.00E-04
HHH	6.3900E-02 ± 3.00E-04	5.4300E-02 ± 3.00E-04	4.7741E-02 ± 3.00E-04
C	1.0250E-01 ± 4.00E-04	1.0430E-01 ± 4.00E-04	1.0411E-01 ± 4.00E-04
CC	2.4500E-02 ± 2.00E-04	2.1790E-02 ± 2.00E-04	1.8937E-02 ± 2.00E-04
CCC	5.3700E-03 ± 8.80E-05	4.4370E-03 ± 8.00E-05	3.5057E-03 ± 7.00E-05
HC	4.8300E-02 ± 3.00E-04	4.5320E-02 ± 3.00E-04	4.1987E-02 ± 2.00E-04
CH	5.0540E-02 ± 3.00E-04	4.3420E-02 ± 2.00E-04	3.7657E-02 ± 2.00E-04
HHC	1.8930E-02 ± 2.00E-04	1.7510E-02 ± 2.00E-04	1.6291E-02 ± 2.00E-04
CHH	2.5410E-02 ± 2.00E-04	2.0360E-02 ± 2.00E-04	1.6660E-02 ± 2.00E-04
HCH	2.4620E-02 ± 2.00E-04	2.1800E-02 ± 2.00E-04	1.9337E-02 ± 2.00E-04
CCH	1.1030E-02 ± 1.00E-04	8.9360E-03 ± 1.00E-04	7.0771E-03 ± 1.00E-04
HCC	9.7830E-03 ± 1.00E-04	9.1510E-03 ± 1.00E-04	8.4100E-03 ± 1.00E-04
CHC	9.3930E-03 ± 1.00E-04	8.1570E-03 ± 1.00E-04	7.0014E-03 ± 1.00E-04
Others	8.3950E-02 ± 3.00E-04	7.6690E-02 ± 3.00E-04	6.8684E-02 ± 3.00E-04

scattering events with at least 1 H scattering are about 2 times larger than single H scattering, and therefore remarkably contribute to the total response.

Fig. 1(a) shows the total pulse height distribution, as well as the pulse height distributions generated by neutron histories that include $n \leqslant 3$ scatterings on H and $m \leqslant 3$ scatterings on C. As expected, the light produced by the collisions on H extends to high-pulse heights, whereas that produced by the collisions on C is limited to low-pulse heights. Note that the histories involving collisions on C only are responsible for the peak at low-pulse heights in the total distribution. The pulse height distributions generated by neutron histories with collisions on both H and C are shown in Figs. 1(b) and (c). Fig. 1(b) shows the pulse height distributions generated by neutron histories with both a single scattering on H and a single scattering on C. The neutron histories for which the H scattering occurs first generate larger pulse heights than those histories for which the C scattering occurs first. This is consistent with the fact that C scatterings generate small amounts of light, while

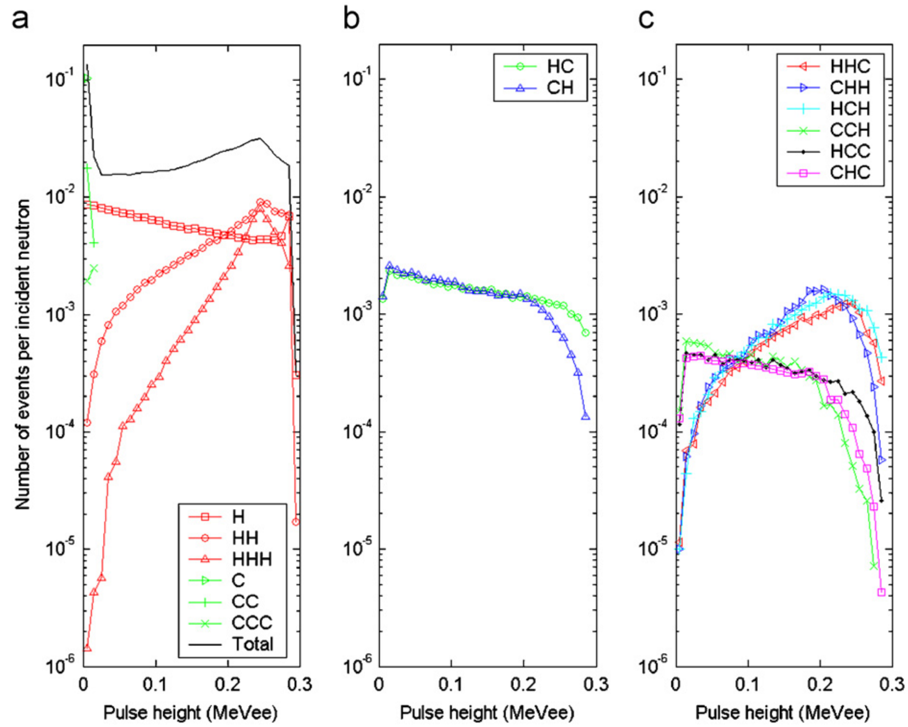

Fig. 2. Pulse height distributions from 1.5 MeV incident neutrons generated by neutron histories with (a) up to three scatterings on H or C only, (b) a single scattering on H and C, and (c) three scatterings on H and C.

reducing the energy of the incident neutron (see Eq. (2)). Fig. 1(c) shows the resulting pulse height distributions for neutron histories comprising of all combinations of 3 scattering events that involve collisions on both H and C. As expected, histories with 2 H scatterings generate consistently more light than the histories with 2 C scatterings.

Fig. 2 shows the pulse height distributions for 1.5-MeV incident neutrons, and Fig. 3 shows the pulse height distributions for 2 MeV incident neutrons. The maximum light output produced by neutron interactions for the 2 MeV incident neutrons now extends up to a value of approximately 0.42 MeVee. This is consistent with the evaluation of Eq. (1) for $T = 2$ MeV, corresponding to the maximum energy deposition on H from neutrons with energy 2 MeV.

Fig. 4 shows the probability of the neutron histories as a function of the number of scatterings on H and C for 1, 1.5, and 2 MeV incident neutrons. For all 3 incident neutron energies, the most probable type of interaction is single scattering on H. For 1 and 1.5 MeV neutron sources, this type of interaction is followed by double scattering on H, single scattering on C, and single scattering on both H and C. For the 2 MeV neutron source, the most probable interactions after single scattering on H are single scattering on C, double scattering on H and single scattering on both H and C.

In the past, the results from the simulations were validated by performing experiments with a BC-501A cylindrical liquid scintillator, a fast waveform digitizer, and two neutron sources: Cf-252 and Am-Be. A description of the experimental setup and validation comparisons are given in [2].

Here we present the analysis of a pulse height distribution from continuous neutron sources. Fig. 5 shows the pulse height distribution for the Am-Be source subdivided into its components on the basis of the number of collisions on H and C that the neutrons underwent in their history. Single scatterings on H are the predominant mechanism of detection at high pulse heights, followed by double and triple scatterings on H. Fig. 6 shows the same pulse height distributions for the Cf-252 source.

4. Analytical approach

Due to the relationship between the deposited energy, T, and the corresponding light, L, for H and C in Eqs. (1) and (2) the distribution of the deposited energy is needed for the calculation of the distributions of the light amplitudes. In the following text, isotropic scattering in the center of mass system is assumed throughout the derivation. This is a correct assumption for scattering on hydrogen at relevant energies, but a simplification in the case of heavier nuclei above 1 MeV. In the case of scattering on H, the distribution of the transferred energy in a collision of a neutron of energy E_0 is given by the relationship

$$p(T, E_0)\, dT = \frac{dT}{E_0}, \tag{3}$$

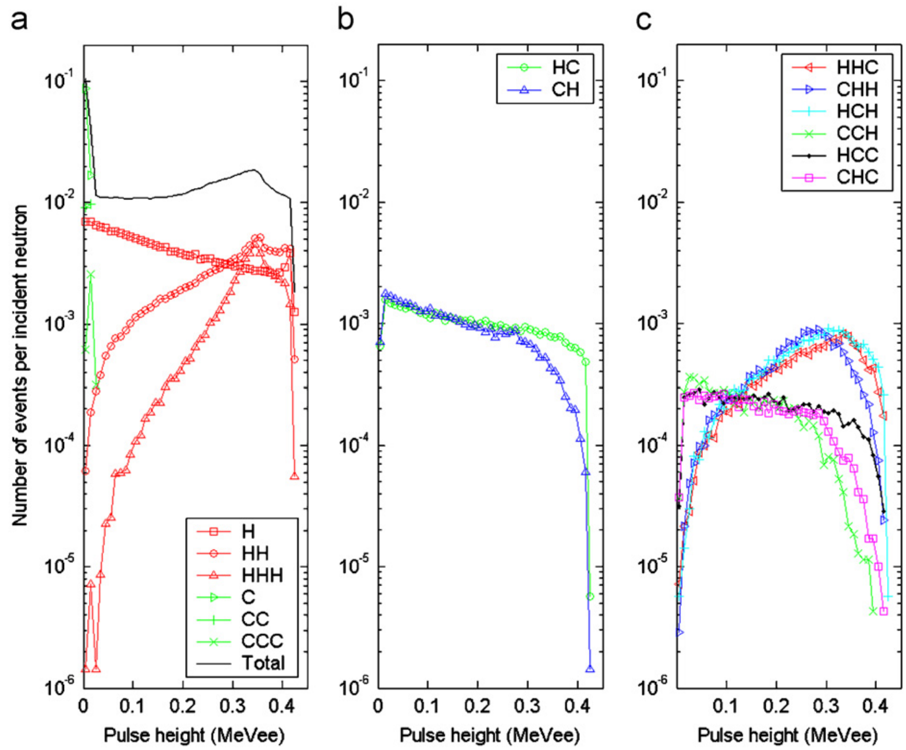

Fig. 3. Pulse height distributions from 2 MeV incident neutrons generated by neutron histories with (a) up to three scatterings on H or C only, (b) a single scattering on H and C, and (c) three scatterings on H and C.

where T ranges from 0 to E_0. In the case of heavier nuclei, T ranges from 0 to $(1-\alpha)E_0$, where for a scattering of a neutron on a nucleus of atomic number A, α is given as

$$\alpha = \frac{(A-1)^2}{(A+1)^2}. \tag{4}$$

From Eqs. (1) and (3), it is possible to calculate the distribution $f_{kX}(L,E_0)$ of the total light generated in k collisions by a single neutron on nucleus X. The sum of light intensities generated in single collisions equals the total intensity of a single light pulse in the detector. To obtain the distribution of $f_{1X}(L,E_0)$, we note that the distribution of T is known, and there is a one-to-one relationship $L(T)$ between transferred energy and induced light. Hence the task is to find the distribution of the function of a random variable with a known distribution. If a second variable, y, is expressed as a single-valued function of x in the form $y=g(x)$, its distribution, $f_y(y)$, is given in terms of the distribution of x as

$$y(y) = \frac{f_x(x)}{|g'(x)|}. \tag{5}$$

Identifying x with the transferred energy and y with the produced light and using the relations in Eqs. (1) and (3) it follows that for collisions on H one has

$$f_{1\mathrm{h}}(L,E_0) = \frac{1}{E_0\sqrt{b^2+4aL}}, \tag{6}$$

for L lying between 0 and $\max,\mathrm{h} = aE_0^2 + bE_0$, and zero for $> aE_0^2 + bE_0$.

From here the distribution of the light generated by multiply collided neutrons can be calculated by convolution-type integrals. The distribution after 2 collisions, $f_{2\mathrm{h}}(L,E_0)$, is given as

$$\begin{aligned} f_{2\mathrm{h}}(L,E_0) &= \int_0^L f_{1\mathrm{h}}(L-l, E_0 - T_\mathrm{h}(l)) f_{1\mathrm{h}}(l,E_0)\,\mathrm{d}l \\ &= \frac{1}{E_0}\int_0^L \frac{1}{(E_0 - T_\mathrm{h}(l))\sqrt{b^2+4a(L-l)}} \\ &\quad \times \frac{1}{\sqrt{b^2+4al}}\,\mathrm{d}l, \end{aligned} \tag{7}$$

where

$$T_\mathrm{h}(l) = \frac{1}{2a}\left\{\sqrt{b^2+4al} - b\right\}, \tag{8}$$

with $T(L)$ being the inverse of $L(T)$. The reason for the convolution integral is that to arrive at a probability distribution for a certain light output one has to sum up the contributions for all possible collisions leading to a total light generation L. This procedure can be continued to find the formula for the light distribution of higher numbers of collisions on H through more complex convolution integrals.

For collisions on C, a similar approach can be used by changing the initial distribution:

$$f_{1\mathrm{c}}(L,E_0) = \frac{\theta(L_{\max,\mathrm{c}} - L)}{\mathrm{c}(1-\alpha)E_0}, \tag{9}$$

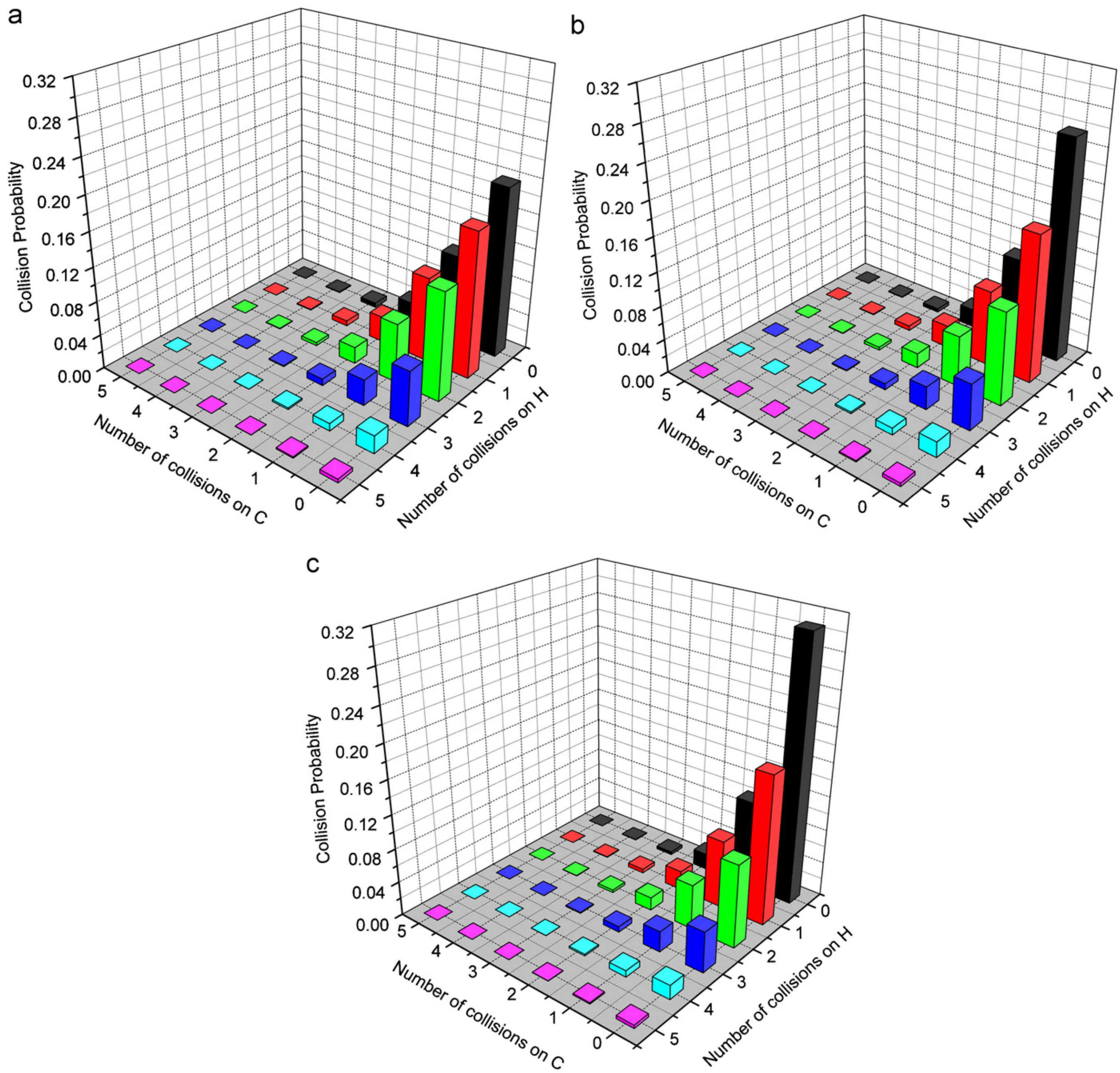

Fig. 4. Probability of neutron histories as a function of the number of scatterings on H and C for (a) 1 MeV incident neutrons, (b) 1.5 MeV incident neutrons, and (c) 2 MeV incident neutrons.

where $\theta(x)$ is the unit step function. Higher-order collisions on C can be expressed in a form similar to Eq. (7) for scattering on H. For the light distribution from scatterings involving both H and C, convolution integrals can be used again. For instance, to express the case of two collisions where the first one is on H and the second on C:

$$f_{\mathrm{hc}}(L, E_0) = \int_0^L f_{1\mathrm{c}}(L - l_1, E_0 - T_{\mathrm{h}}(l_1)) f_{1\mathrm{h}}(l_1, E_0)\,\mathrm{d}l_1. \tag{10}$$

On the other hand, for collisions in the reverse order, the pulse height distribution can be calculated as

$$f_{\mathrm{ch}}(L, E_0) = \int_0^L f_{1\mathrm{h}}(L - l_1, E_0 - T_{\mathrm{c}}(l_1)) f_{1\mathrm{c}}(l_1, E_0)\,\mathrm{d}l_1. \tag{11}$$

When plotting the different collision histories involving both H and C, the order of scatterings has a significant effect on the pulse height distribution. This can also be seen in the separate distributions from collision histories

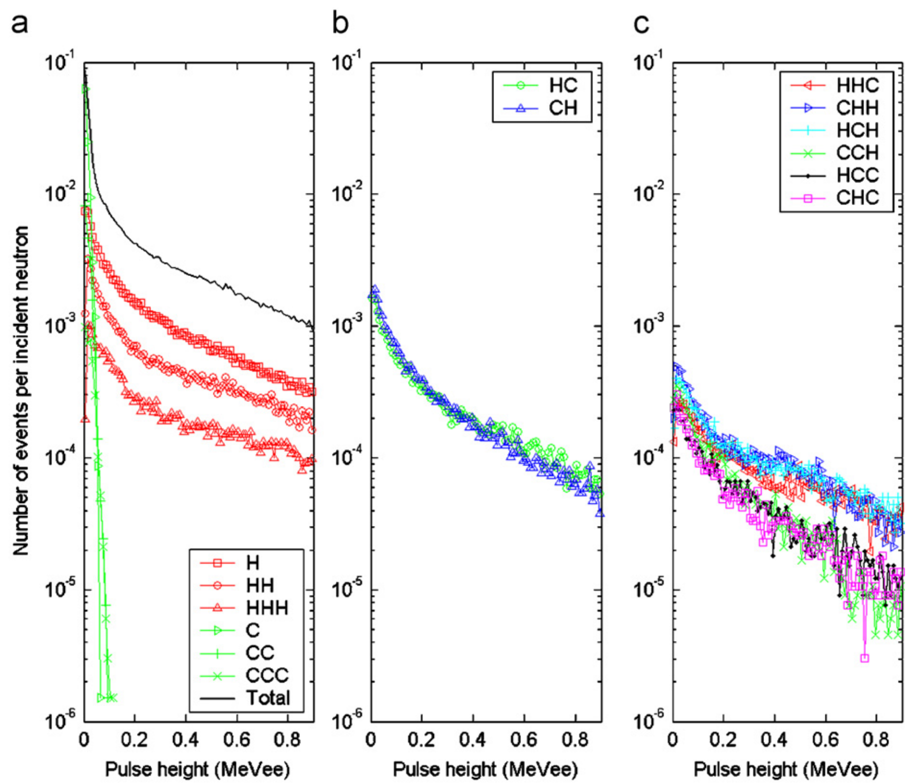

Fig. 5. Pulse height distributions from Am-Be source generated by neutron histories with (a) up to three scatterings on H or C only, (b) a single scattering on H and C, and (c) three scatterings on H and C.

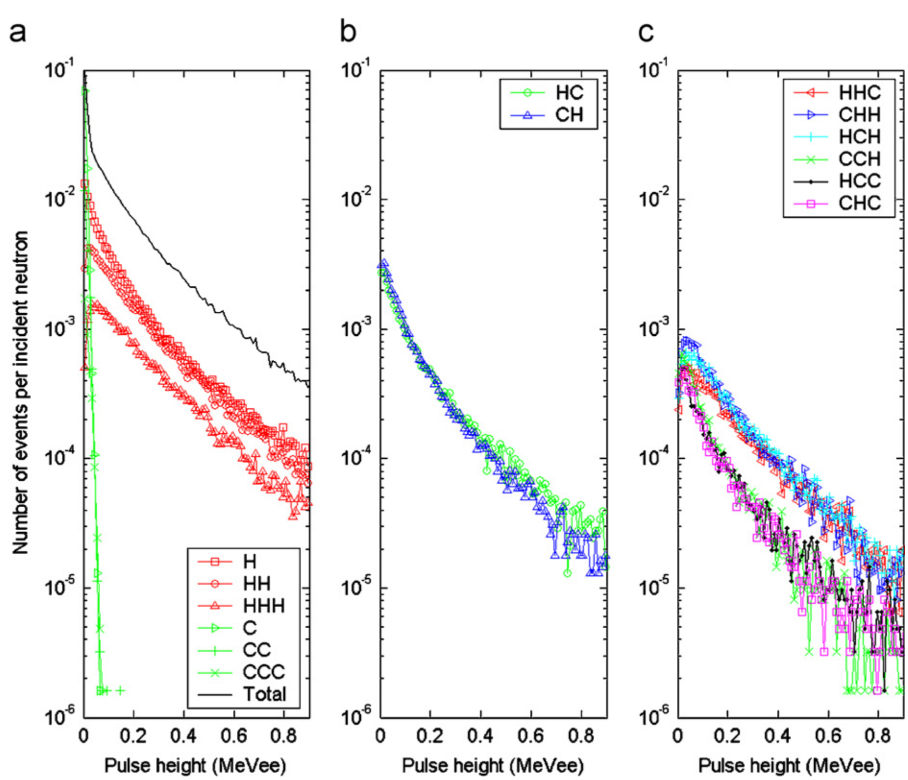

Fig. 6. Pulse height distributions from Cf-252 source generated by neutron histories with (a) up to three scatterings on H or C only, (b) a single scattering on H and C, and (c) three scatterings on H and C.

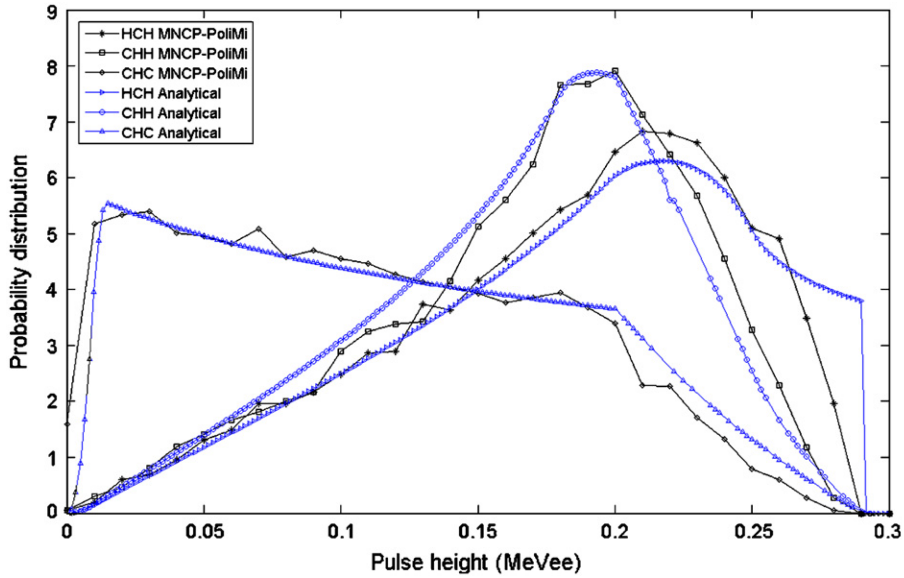

Fig. 7. Pulse height distributions from 1.5 MeV incident neutrons generated by neutron histories with three scatterings on H and C. Comparison between the analytical results and the MCNP-PoliMi simulations is shown.

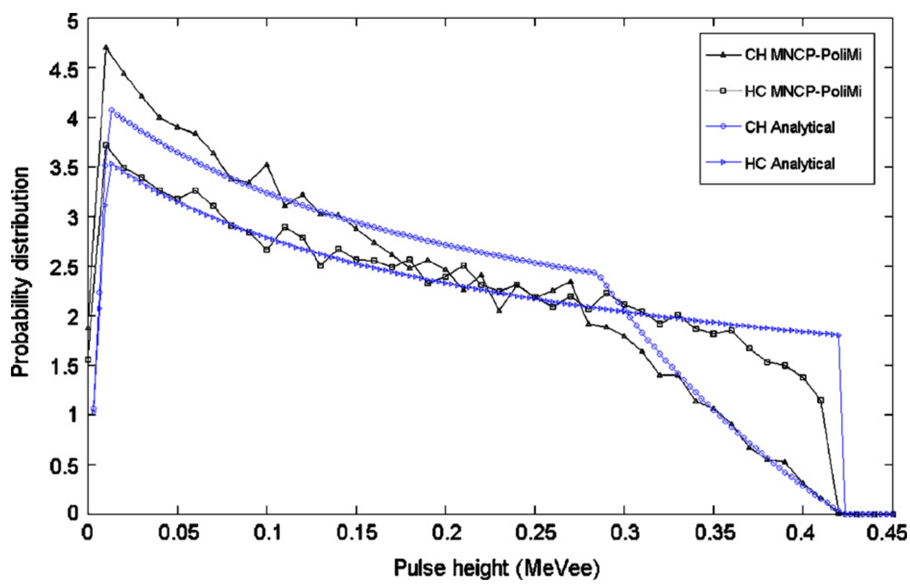

Fig. 8. Pulse height distributions from 2 MeV incident neutrons generated by neutron histories with one scattering on H and C, respectively. Comparison between the analytical results and the MCNP-PoliMi simulations is shown.

calculated by using MCNP-PoliMi. Figs. 7 and 8 show comparisons between the simulated and analytically-calculated pulse height distributions for incident neutron energies equal to 1.5 and 2.0 MeV. Good agreement is observed between the result obtained from the simplified analytical model and those obtained with the sophisticated Monte Carlo simulations.

5. Conclusions

This paper describes a new technique based on the Monte Carlo approach, and an analytical approach, to analyze the statistics of neutron interactions with organic scintillation detectors. Neutron histories were analyzed according to the number and order of collisions on hydrogen and carbon, the main constituents of the organic scintillators. The detection statistics of neutrons from a monoenergetic source and from two continuous energy sources, Am-Be and Cf-252, were determined. The total pulse height distributions obtained with the simulations were compared with experimental data and good agreement was obtained. The pulse height distributions given by specific neutron histories were compared with the results from the analytical model, and very good agreement was obtained.

The methodology presented in this paper can be applied to techniques such as neutron spectrum unfolding, which has a variety of applications, including nuclear nonproliferation and homeland security.

Acknowledgments

The Oak Ridge National Laboratory is managed and operated for the US Department of Energy by UT-Battelle, LLC, under Contract DE-AC05-00OR22725. This work was supported in part by the US Department of Energy, National Nuclear Security Administration Office of Nonproliferation Research Engineering, NA-22. We thank the reviewers for detailed and insightful comments on this manuscript.

References

[1] G.F. Knoll, Radiation Detection and Measurement, third Ed., Wiley, New York, 2000, p. 555.
[2] M. Flaska, S.A. Pozzi, Nucl. Instr. and Meth. A 577 (2007) 654.
[3] H. Klein, S. Neumann, Nucl. Instr. and Meth. A 476 (2002) 132.
[4] D.L. Smith, R.G. Polk, T.G. Miller, Nucl. Instr. and Meth. 64 (1968) 157.
[5] M. Drogs, Nucl. Instr. and Meth. 105 (1972) 573.
[6] R.A. Cecil, B.D. Anderson, R. Madey, Nucl. Instr. and Meth. 161 (1979) 439.
[7] J.L. Fowler, J.A. Cookson, M. Hussain, R.B. Schwartz, M.T. Swinhoe, C. Wise, C.A. Uttley, Nucl. Instr. and Meth. 175 (1980) 449.
[8] R.L. Craun, D.L. Smith, Nucl. Instr. and Meth. 90 (1970) 239.
[9] V.V. Verbinski, W.R. Burrus, T.A. Love, W. Zobel, N.W. Hill, Nucl. Instr. and Meth. 65 (1968) 8.
[10] C. Bähr, R. Böttger, H. Klein, P. von Neumann-Cosel, A. Richter, D. Schmidt, K. Schweda, S. Strauch, Nucl. Instr. and Meth. A 411 (1998) 430.
[11] K. Schweda, D. Schmidt, Nucl. Instr. and Meth. A 476 (2002) 155.
[12] J.K. Dickens, SCINFUL-A Monte Carlo-Based Computer Program to Determine a Scintillator Full Energy Response to Neutron Detection for Energies between 0.1 and 80 MeV: User's Manual and FORTRAN Program Listing, ORNL Report 6462, March 1988.
[13] D. Hermsdorf, K. Pasieka, D. Seeliger, Nucl. Instr. and Meth. 107 (1973) 259.
[14] S.A. Pozzi, E. Padovani, M. Marseguerra, Nucl. Instr. and Meth. A 513 (2003) 550.
[15] S.A. Pozzi, J.A. Mullens, J.T. Mihalczo, Nucl. Instr. and Meth. A 524 (2004) 92.